THE OHIO STATE UNIVERSITY

William G. Lowrie Department of Chemical and Biomolecular Engineering

Undergraduate Honors Research Thesis

Modifying the Catalytic Activity of Zeolite-based Catalysts using Morphology Control

Justin Hopkins

PI: Dr. Nicholas Brunelli

Submitted: April 2nd, 2021

Email: hopkins.810@buckeyemail.osu.edu

Abstract

Porous heterogeneous catalysts are driving an evolution in catalysis because they have enabled unprecedented catalytic chemistry. However, these porous materials are plagued by mass transfer limitations wherein the reactants have difficulty diffusing to the catalytically active sites where the chemistry occurs. As a result, researchers have pushed to create nanoparticle catalysts like nanozeolites that achieve shorter path lengths from the bulk solution to active sites at the cost of decreased ease of separation. In contrast, our work seeks to control the morphology by modifying the growth of specific faces of micron-sized zeolite catalysts. In this way, we hypothesized that these morphology-controlled zeolites would exhibit shorter path lengths to active sites and superior catalytic activity while avoiding the separation challenges posed by nanoparticles.

In this study, we synthesized Sn-substituted zeolite MFI catalysts using an additive known to increase the plate-like character of MFI crystals, called spermine. Ultimately, we engineered Sn-MFI catalysts with and without spermine under hydrothermal synthesis conditions. After synthesis, we characterized the materials' crystallinity using XRD and the porosities using N2 physisorption. Upon confirmation of successful syntheses, we tested these catalysts in the epoxide-ring opening reaction of 1,2-epoxyhexane using methanol. We compared the epoxide reactant conversion of the modified and non-modified zeolite catalysts at various time points. Thereby, we determined the effects of the crystal modifications on these materials' catalytic activities. Ultimately, these materials had similar catalytic activities as compared to non-modified samples.

Contents

List of Figures

List of Tables

Background

Catalysis has revolutionized the chemical processing industry by transforming unproductive reactions into viable chemical pathways. For example, tertiary amines were shown to have high catalytic activity in the isomerization of glucose to fructose [1]. In this reaction, tertiary amines were dissolved in the reactant mixture, and the reaction took place in the same aqueous phase as the catalyst. Catalysis occurring in the same phase as the reaction, like tertiary amine-catalyzed glucose isomerization, is known as homogeneous catalysis. Despite the promise of homogeneous catalysis, these catalysts are often difficult to separate since they are in the same phase as the reactants and products [2]. This challenging separation makes homogeneous catalysts difficult to incorporate in industrial processes since their reuse relies on expensive and energy-intensive methods to separate them from solution.

In contrast, a heterogeneous catalyst exists in a different phase than the reaction. Typically, the catalyst is a solid or is solid-supported, and the reaction taking place in a liquid or gas phase. Because of the difference in phases, heterogeneous catalysts are easier to separate using solids separations processes such as vacuum filtration [2]. In some cases, chemical groups that catalyze desired reactions are first discovered as homogeneous catalysts [3]. These chemical groups can then be translated to heterogeneous catalysts by immobilizing these groups on solid-supports while maintaining the ease of separation. For example, heterogeneous V-Sb bimetallic catalysts enabled the oxidative ammoxidation of propene [4]. This heterogeneous catalyst revolutionized the production of acrylonitrile. Because of their solid nature, these bimetallic catalysts were able to operate in a fluidized bed reactor where the catalyst was trapped. The ability to incorporate the catalyst into a fluid bed allowed for continuous use of the catalyst. Therefore, heterogeneous catalysis has allowed us to combine the catalytic functionality of chemical groups with facile separation techniques making them favored in large-scale chemical processing.

Additionally, porous catalysts and catalyst supports like zeolites and SBA-15 materials provide the opportunity to incorporate catalytic groups in a stable framework [5]. The entrapment of these chemical groups in a network of pores allows us to create catalytic environments in large surface area materials. For example, tertiary amine-grafted SBA-15 proved to possess lower catalytic activity in glucose isomerization than homogeneous tertiary amine catalysts [6]. However, the ability to immobilize the amines on the SBA-15 surface allowed for easier separation and reuse of these catalysts while allowing for high surface area for grafting. Additionally, the microporosity of zeolite-based catalysts can serve as molecular sieves as well [7]. Sn-substituted MFI (Sn-MFI) zeolites were shown to modify the selectivity

of bulkier products in the epoxide ring-opening reaction [5]. Thereby, Sn-MFI catalyzes these reactions in a controlled fashion to control the selectivity. Overall, porous catalyst supports like SBA-15 and zeolites allow for the immobilization of traditionally homogeneous catalytic groups in a heterogeneous pore network.

However, microporous materials like zeolites can be plagued by diffusion limitations [5]. As reactants and products accumulate in the pores, the mass diffusivity of these materials declines. Because of this, the ability to transport reactants to catalytic active sites decreases. Therefore, the catalytic activity of these materials appears to decline as the reaction proceeds. Much research is devoted to decreasing these mass transfer limitations in porous catalysts. The goal of these techniques is to decrease the path length from the bulk solution to the catalyst's active site. If this research is fruitful, the activity of porous catalysts can be maintained over the span of the reaction making them more viable in large-scale chemical processing.

One viable route is to decrease the size of bulk zeolite crystals. By creating nanozeolites, the path lengths from the bulk solution to the active sites are decreased significantly. For example, Brunelli et al. showed that the catalytic activity and overall access to active sites increased when using nano-Sn-MFI catalysts compared to conventional Sn-MFI catalysts [8]. However, due to their small crystal size, these materials must be separated from the mixture using more difficult separation techniques like centrifugation.

In contrast, techniques have been developed that attempt to change the aspect ratio of the crystal dimensions. Researchers have identified ways to control the morphology of zeolite crystals by either making adjustments to synthesis formulas or by adding organic modifiers to the syntheses. In this way, one dimension becomes thinner in comparison to the conventional zeolite structure. Thereby, the modification decreases the diffusion path length to active sites therefore decreasing the diffusion limitations within these materials.

For example, Valtchev et al. controlled the morphology of zeolite BEA by varying the amount of fluoride used in the synthesis solution [9]. They used a specialty fluorinated silica precursor (SiF_6^-)in conjunction with the structure-directing agent (SDA), tetraethylammonium hydroxide (TEAOH), in their synthesis. They found that increased concentrations of the SiF_6^- in the synthesis resulted in taller zeolite BEA crystals. In contrast, Rimer et al. used organic modifiers to demonstrate morphology control of multiple zeolite structures [10, 11]. In their work, Rimer et al. identified over 25 different organic zeolite growth modifiers (ZGMs) for zeolite LTL [10]. They studied the change in the aspect ratio of zeolite LTL based on the ZGM used and noted that glycerol increased the aspect ratio the most to create longer, thinner LTL crystals. They also found that 1,2,3-hexanetriol decreased the aspect ratio the most to yield shorter, thicker crystals.

Additionally, these same groups have demonstrated morphology control on zeolite MFI, a zeolite commonly used in the chemical and petroleum industry. Valtchev et al. extended their work on zeolite BEA to zeolite MFI recently [12]. They similarly showed that using fluoride-assisted crystallization allowed them to reduce a single crystal dimension of zeolite MFI in all-silica forms and with Al- and Ga-substituted forms. Additionally, they demonstrated that Al-MFI (also known as ZSM-5) shows superior catalytic activity than commercially available nano-ZSM-5. Additionally, Rimer et al. also demonstrated the ability of ZGMs to alter the morphology of all-silica MFI (Si-MFI) crystals [11]. In this work, they identified spermine as an excellent ZGM capable of yielding thinner Si-MFI crystals. In fact, they demonstrated using scanning electron microscopy (SEM) that synthesis solutions of 0.5 weight % spermine or lower were capable of yielding this change in morphology.

In this study, we extended the work of Rimer et al. on zeolite MFI. Spermine was used to generate crystalline Si-MFI and Sn-substituted MFI. Following successful syntheses, we compared the catalytic activity of the Sn-MFI samples synthesized with and without spermine using the epoxide ring-opening reaction of 1,2-epoxyhexane in excess methanol. Sn-MFI catalysts have become less catalytically active over the duration of the reaction due to diffusion limitations and pore blockage that increases as the reaction proceeds. Therefore, we hypothesize that Sn-MFI synthesized with 0.5 weight % spermine will have superior catalytic activity and fewer diffusion limitations than Sn-MFI synthesized without spermine.

Experimental Description

Chemicals Used

To synthesize zeolite MFI, we used tetraethyl orthosilicate (TEOS, 98%, Acros Organics) as the silica source. To aid in the formation of MFI, we used tetrapropylammonium hydroxide (TPAOH as ZeoGen SDA 746, 40% in H_2O, SACHEM Inc.) as the structure directing agent (SDA). For Sn-MFI syntheses, we added $SnCl_4$ hydrate (98%, Alfa Aesar) to the synthesis solutions. For use as a ZGM, we used spermine (97%, Acros Organics). During kinetic testing of the synthesized catalysts, we used 1,2-epoxyhexane (97%, Acros Organics). Additionally, we used diethylene glycol dibutyl ether (DGDE, 98%, TCI) as an external GC-FID standard during kinetic testing.

Zeolite Synthesis

To prepare conventional Si-MFI, we created synthesis solutions with molar ratios with SiO_2, TPAOH, H_2O, and ethanol. The SiO_2 and ethanol were liberated through the hydrolysis of TEOS, described by TEOS + $2\,H_2O \longrightarrow SiO_2$ + 4 ethanol. Similarly, we synthesized conventional Sn-MFI using a Si:Sn ratio of 1:0.005 and SiO_2, TPAOH, H_2O, and ethanol. Following the procedures of Rimer et al., we first synthesized zeolite MFI under very dilute conditions with 1 SiO_2: 233 H_2O. For Sn-MFI synthesized under dilute concentrations, the ratio of Si:Sn was kept at 1:0.005. Finally, we performed moderate concentration syntheses with concentrations of 1 SiO_2: 55.6 H_2O. Again, Si:Sn ratios of 1:0.005 were used in Sn-MFI syntheses under moderate concentrations. When spermine was used in syntheses, we always added it to achieve a total solution (including H_2O) spermine % of 0.5%. Table 1 below shows the molar ratios of reagents used in these syntheses. Table 3 in Appendix A shows the masses of these chemicals used in the syntheses.

Table 1: Zeolite MFI synthesis reagent ratios.

Synthesis Concentration	**SiO_2: TPAOH**	**SiO_2:H_2O**	**SiO_2:ethanol**
Conventional	0.36	19.2	4
Dilute	1.00	233	4
Moderate	0.24	55.6	4

To create the synthesis solutions for Si-MFI, we added TEOS to a round bottom flask with a stir bar. TPAOH and H_2O were mixed separately before adding them to the TEOS. Once well-mixed, we added the TPAOH-H_2O solution semi-dropwise to the TEOS mixture. An emulsion of TEOS-H_2O was often formed with the first 5-10 mL of added TPAOH-H_2O. As more TPAOH-H_2O was added and the mixture was stirred with the stir bar, the mixture became homogeneous and gained a translucent white color. The contents of the flask were allowed to react for 20-24 hours. After this period of hydrolysis, the solution was fully transparent. For Si-MFI samples synthesized without spermine, this solution was then transferred to a Parr reactor. For samples that were to be synthesized with spermine, we added spermine to the samples after the hydrolysis period to achieve a total solution weight % of spermine of 0.5%. In these cases, the spermine was allowed to dissolve for 15 minutes before we transferred the solution to a Parr reactor.

To create Sn-MFI synthesis solutions, $SnCl_4$ was dissolved in the TEOS for 30 minutes before adding the TPAOH-H_2O. After this period, the $SnCl_4$ was well dissolved. Upon adding TPAOH-H_2O, a precipitate would initially form in the mixture. However, after all of the

TPAOH-H_2O had been added, the precipitate would redissolve. The solution was allowed to hydrolyze for 20-24 hours. We then transferred the solution to a Parr reactor after this period for samples without spermine. For samples with spermine, we allowed the spermine to dissolve in the solution for 15 minutes before being transferred to a Parr reactor.

For conventional Si-MFI and Sn-MFI, we made synthesis solutions of about 20 mL with a maximum yield of zeolite of 1.78 g. We transferred these solutions to a 48-mL Teflon-lined Parr reactor and sealed them. For dilute Si-MFI and Sn-MFI samples, we made synthesis solutions in both 24-mL amounts with a maximum yield of 0.30 g and 100-mL amounts with a maximum yield of 1.29 g. Due to the larger solution size, we transferred these synthesis solutions to 200-mL Parr reactors and sealed. We made the moderate concentration Si-MFI and Sn-MFI in 24-mL amounts with maximum yields of 1.11 g. We sealed these solutions in 48-mL Parr reactors. All Parr reactors were placed in an oven at 160 ^{o}C without rotation. We left the conventional Si-MFI and Sn-MFI in the oven for over 100 days due to COVID-19 shutdown from March 2020 until June 2020. We left the dilute Si-MFI and Sn-MFI samples in the oven for upwards of 20 days. We left the moderate concentration samples in the oven for at least 3 days.

The reactors were removed from the oven and cooled with flowing cold water. Once cooled, we filtered the solids from the solution. For the dilute Si-MFI and Sn-MFI solutions, the crystals were large enough to filter solely using vacuum filtration. We rinsed the crystals thoroughly to ensure adequate removal of the SDA, ZGMs, and contaminants from the crystals. For the conventional and moderate concentration syntheses, a fraction of the crystals were too small to filter with vacuum filtration. We filtered the solids using 10 minutes of centrifugation at 9000 rpm followed by decantation. Multiple rounds of centrifugation, decantation, and distilled H_2O rinsing were performed until the supernatant solution was pH-neutral. A pH-neutral solution indicated the removal of the basic SDA and spermine. Following both filtration techniques, we dried the solids in a vacuum oven at 80 ^{o}C.

Once dried, we removed any remaining organic contaminants in the zeolite pores using calcination. To do so, the solids were placed in a ceramic dish inside a calcination oven. The oven was ramped from room temperature to 550 ^{o}C in 4 hours and 52 minutes. The oven was held at 550 ^{o}C for 10 hours to ensure the combustion of any organic contaminants. After this period, the oven temperature was decreased to room temperature in 4 hours and 18 minutes. Following calcination, all materials were white powder.

Characterization of Materials

We used multiple characterization techniques to determine if the syntheses were successful in forming zeolite MFI. Firstly, we used X-ray diffraction (XRD) to probe the crystallinity of the zeolites synthesized. The XRD patterns recorded were compared directly to confirmed syntheses of zeolite MFI. Similarly, the pore dimensions were calculated using N_2 physisorption data. The synthesized zeolites' surface area per mass of material was compared to those of confirmed MFI syntheses.

XRD enables us to determine the crystalline characteristics of the materials. In this technique, X-rays are aimed at the powder surface at controlled angles. These angles are referenced as 2θ where θ is the angle between the powder surface and incident X-rays. The crystal facets diffract X-rays at various intensities at each angle. Interestingly, each unique crystalline material will characteristically diffract the X-rays. By comparing the intensity versus 2θ graphs of our synthesized materials to those of confirmed MFI materials, the zeolite can be determined to be consistent with crystalline MFI. In specific, we measured scattering intensity over the 2θ range of 5^o to 50^o, and we normalized all intensity values. In this study, XRD was performed on materials before calcination.

To characterize the porosity of the synthesized zeolites, we used N_2 physisorption. Due to the microporosity of zeolites, fully crystalline materials adsorb N_2 primarily at low relative pressures [13]. In N_2 physisorption, an evacuated tube with our sample is injected with known amounts of N_2. Throughout the process, the sample is cooled to 77 K with liquid N_2. The N_2 will then either adsorb to the zeolite surfaces or stay within the gas phase and contribute to gaseous pressure. By measuring the quantity of N_2 added to the tube, the amount of N_2 adsorbed can be calculated. The adsorption of N_2 occurs via a multilayer adsorption mechanism [14]. We then used Brunauer–Emmett–Teller (BET) theory to calculate the surface area per mass of the materials. Using these calculated values, we can compare the porosity of our zeolites. Thus, we further confirmed the successful synthesis of these materials using N2 physisorption.

Kinetic Testing Procedure

With the incorporation of Sn into the MFI framework, the zeolite materials can conduct Lewis acid catalysis. Therefore, we tested these materials in the epoxide ring-opening reaction to probe the ability of the synthesized Sn-MFI materials. Specifically, we used 1,2-epoxyhexane for trials on the materials synthesized for this study. Methanol was reacted with the epoxide to produce a terminal ether and a terminal alcohol product according to the reaction scheme shown in Figure 1. We used this reaction to understand the catalytic activity of our materials.

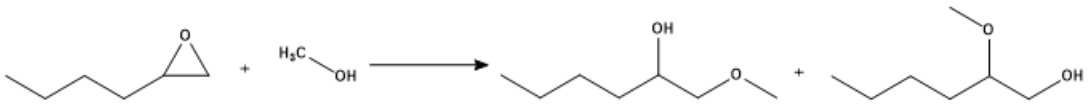

Figure 1: The epoxide-ring opening reaction scheme of 1,2-epoxyhexane with methanol.

In this study, we conducted kinetic testing at 60 deg C in a silicone oil bath. We prepared a solution of 2.00 mL of methanol, 20 μL of diethylene glycol dibutyl ether (DGDE), and 98 μL of 1,2-epoxyhexane for each trial. The DGDE served as an external standard for the gas chromatography (GC) process. The amount of epoxide added corresponds to a 0.4 M solution. Theoretical Si:Sn ratios of 200:1 were assumed. Therefore, we added 0.0385 g of the calcined zeolite catalyst to produce a theoretical molar ratio of epoxide:Sn of 250:1. The round-bottom flask containing the materials was outfitted with a 14/20 condenser and septa to create a closed system. We circulated room temperature water through the condenser to condense any volatile components, including the methanol reactants, epoxides, and products. A small stir bar stirred the resulting solutions at 600 rpm. Using this setup, we assume our reactor is batch, well-mixed, constant volume, and constant temperature. Additionally, the excess methanol allows us to assume first-order chemical kinetics with respect to the epoxide.

Once we added the methanol, DGDE, and 1,2-epoxyhexane to the flask, we stirred them for at least two minutes. We took two 40-μL samples before the catalyst was added. We added these to a GC vial and diluted it with acetone until it was 75% full. Following this, we added the catalyst, and we added the round bottom to the condenser system and sealed it. We started a timer at this point. We sampled the reaction solution at 15 minutes, 30 minutes, 1 hour, 2 hours, 4 hours, 7 hours, and 24 hours after this. Sampling was completed with a 20-gauge, 6-inch steel needle fitted with a 1-mL plastic syringe. We sampled approximately 40 μL at each time point. We then filtered these samples through an acetone-wetted silica filter in a 6-inch glass pipette. We rinsed the needle with acetone and enough acetone was added to pipette filter to fill the GC vial 75% full.

Following collection, we analyzed the samples using GC. In this technique, a liquid sample is vaporized and carried through a silica column (stationary phase) using He gas (mobile phase). Based on the affinity of the various components in the samples for the stationary phase, the components will be transported through the column at different rates. More interactive components will spend more time in the column, while components with less affinity for the column will require less time to move through the column. Following the splitting within the column, the outlet is sent through a flame ion detector (FID). In this unit, the outlet stream of the GC column is ionized and detected. The combined output of the GC-FID is a graph

of FID intensity over time. The two most intense peaks corresponded with the two most abundant components of the sample: acetone and methanol. The remaining peaks belonged to 1,2-epoxyhexane, the two reaction products (if present), and DGDE. The relative intensity of the epoxide and products changed as the reaction proceeds. However, the reaction solution samples were not exactly 40 μL. However, DGDE's concentration in the sample should be constant since it does not react in this system,. Therefore, the GC-FID intensity ratio of epoxide to DGDE was used to calculate the epoxide concentration in the reaction flask at each time point, assuming exactly 0.4 M epoxide initially. The concentration was calculated by taking the ratios of the 1,2-epoxyhexane : DGDE at each time to the same ratio at the initial time point. Assuming first-order kinetics in a well-mixed batch reactor, Equation 1 describes the unsteady state accumulation of 1,2-epoxyhexane over time.

$$\frac{dc_{EpHex}}{dt} = -kc_{EpHex} \tag{1}$$

The concentration of 1,2-epoxyhexane is dependent upon the amount of it initially added. A more useful value used to monitor the reaction over time is the fractional conversion. To calculate the conversion of 1,2-epoxyhexane over time, the ratio of the amount of it reacted is divided by the initial amount. By assuming first-order reaction kinetics, the fractional conversion (θ_{EpHex}) follows Equation 2 below.

$$\theta_{EpHex} = 1 - exp(-kt) \tag{2}$$

By calculating the conversion for each data point, we were able to fit the data to this equation. Because of diffusion limitations within the synthesized zeolites, we expected our data to deviate to lower conversions over time. Therefore, when fitting purely first-order kinetics, only data up to 1 hour was used to fit the first-order rate constant, k. These rate constants were fit using nonlinear least-squares regression using conversions directly as residuals (e) such that $e = (\theta_{EpHex} - \theta^*_{EpHex})^2$. This fitting method is recommended so that the model errors remain normally distributed with respect to concentration and conversion [15].

Results and Discussion

Dilute Concentration Syntheses

To directly reproduce the work of Rimer et. al, we used synthesis ratios of 1 SiO_2 : 1 TPAOH : 233 H_2O : 4 ethanol. Initially, we made 24-mL batches with a maximum possible yield of 0.30

g. Low concentrations of SiO_2 require large batches to produce sufficient yield. By limiting the concentration of SiO_2, nucleation events are less likely [16]. However, crystallization rates are increased in contrast. The SiO_2 : TPAOH ratios used were very high in comparison to conventional MFI syntheses. Interestingly though, syntheses of higher SDA content have been shown to increase the number of nucleation events, but decrease the size of the crystals as a result [17]. As a result, we expected the low concentration, high SiO_2 : TPAOH syntheses to yield fewer but larger crystals. Rimer et. al discussed that this ratio produced crystals large enough to analyze with SEM.

Rimer et al. left their solutions in a 160 ^oC oven for 2.5 days. However, we found that no noticeable amount of solids could be isolated from this solution after 3 days. Therefore, we repeated the synthesis and kept the reactors in the oven for 11 and 16 days, and a small amount of sample was collected in each synthesis. All samples were separated using vacuum filtration. Following these syntheses, XRD was performed and is shown in Figure 2 below.

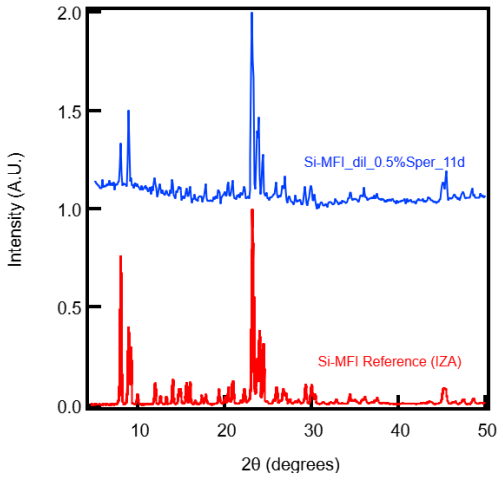

Figure 2: XRD pattern of Si-MFI with 0.5 wt% spermine (blue) versus an International Zeolite Association reference pattern (red) [18]

.

The characteristic peaks of MFI are between 2θ of 7-9^o and 23-25^o [19]. Our sample showed a non-constant baseline because the XRD sample holder interfered with the small amount of solids recovered from the synthesis. The pure sample holder pattern was obtained by performing XRD without any sample in the holder. This pattern was then subtracted out of the sample XRD pattern during data analysis. However, the characteristic peaks were all present. Therefore, the XRD pattern suggests that we formed Si-MFI properly. However, there was insufficient mass of Si-MFI to perform N_2 physisorption.

At the same time, Sn-MFI without spermine were synthesized. These batches employed a synthesis solution that had a molar ratio of 1 SiO_2 : 1 TPAOH : 233 H_2O : 4 ethanol : 0.005 $SnCl_4$. At the time of the synthesis, we discovered that longer syntheses had yielded enough Si-MFI for XRD. Therefore, a 24-mL batch of Sn-MFI without spermine was synthesized at 160 ^oC oven for 14 days. Similar to the Si-MFI samples, only a small amount of solids were recovered. The XRD pattern for this synthesis is shown below in Figure 3.

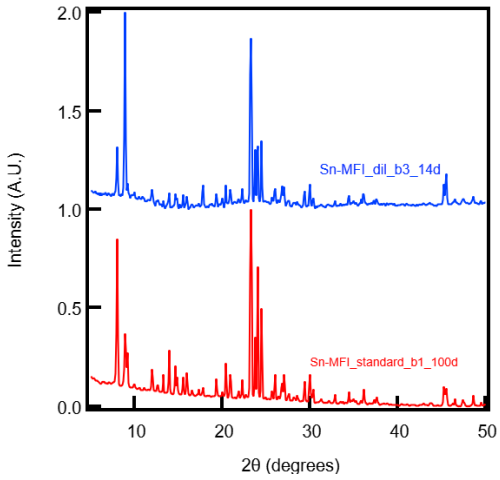

Figure 3: XRD pattern of Sn-MFI synthesized in dilute concentrations (blue) versus conventional Sn-MFI (red).

Similar to Si-MFI, Sn-MFI has very similar characteristic peaks between 7-9^o 2θ and 23-25^o 2θ. However, Sn-MFI has higher relative intensities in the 7-9^o. The reference pattern shown in Figure 3 is a conventional Sn-MFI sample synthesized in March 2020 and left in the oven for over 100 days during the initial COVID-19 shut-down. Since only a small amount of solids were recovered, the XRD sample holder interfered with the XRD and had to be subtracted out of the sample pattern during data analysis. Similar to the Si-MFI sample, there was not enough Sn-MFI sample to perform N_2 physisorption.

To increase the yield of zeolite from the reactors, we began synthesizing solutions of 100 mL and using 200-mL Parr reactors. Using the same synthesis solution ratios, we synthesized an additional large batch of Si-MFI with 0.5 wt% spermine and a large batch of Sn-MFI without spermine. We placed the Si-MFI with 0.5% spermine reactor in a 160 ^oC oven for 22 days, and we then filtered it via vacuum filtration. This batch of Si-MFI with 0.5% spermine yielded 0.12 g of zeolite for a yield of 9%. A summary of each batch of zeolites produced is shown in Table 4 Appendix A. The Sn-MFI reactor was placed in the 160 ^oC oven, resulting in a total oven time of 58 days. In contrast to the large Si-MFI batch sample, about 0.70 g of Sn-MFI was collected from this large batch. This equates to about 54% yield.

To confirm that spermine was not causing lower yields, we also synthesized a large batch of Si-MFI without spermine. We added a 100-mL batch using the synthesis ratio of 1 SiO_2 : 1 TPAOH : 233 H_2O : 4 ethanol to a 200-mL Parr reactor for 41 days. When the reactor was removed from the oven, there was a hard, white solid crusted to the Teflon of the reactor walls. Despite our best effort, the white solid could not be removed without damaging the reactor. We thoroughly cleaned the reactor multiple times by adding KOH to the reactor and placing it back into the 160 ^{o}C oven for 3 days.

Moderate Concentration Syntheses

Since low yields were achieved with the dilute synthesis concentrations of 1 SiO_2 : 233 H_2O, we decided to use a synthesis solution with higher concentration. Rimer et. al suggested that a synthesis ratio of 1 SiO_2 : 0.24 TPAOH : 55.6 H_2O : 4 ethanol provided better yield, but smaller crystals [11]. Additionally, communication with the Rimer group showed that we should continue to maintain the total spermine concentration of 0.5 weight % despite the increase in SiO_2 concentration. This new ratio not only showed an increase in concentration but also showed a decrease in the SiO_2 : TPAOH ratio. Work within the Brunelli research group has shown that increased zeolite yields are observed for lower SiO_2 : TPAOH ratios. Therefore, we expected increased yields from this synthesis solution.

To begin testing this new synthesis ratio, we produced Si-MFI without spermine. We produced two batches of synthesis solution as described in the Experimental Description. The first batch was placed in the 160 ^{o}C oven for 3 days. After this period, we first filtered the reactor contents using vacuum filtration. However, only a fraction of the reactor contents were captured by the filter paper. Therefore, we centrifuged the remaining solution for 10 minutes at 9000 rpm. We dried the solids in a vacuum oven at 80 ^{o}C. The second batch remained in the oven for 17 days. Once removed from the oven, we separated this sample with centrifugation only. The XRD patterns measured for both batches are shown below in Figure 4.

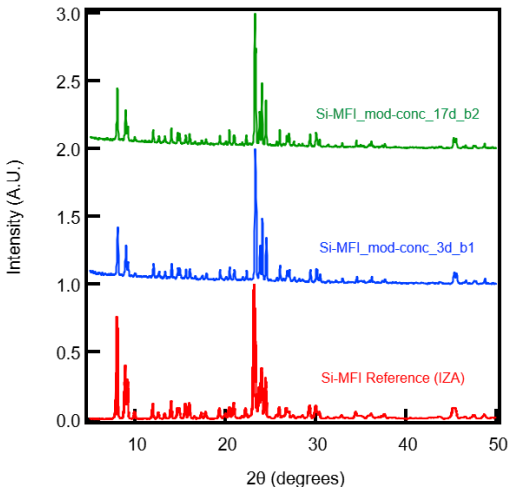

Figure 4: XRD patterns of batch 1 (blue) and batch 2 (green) of Si-MFI under moderate synthesis concentrations compared against conventional Si-MFI (red) [18].

As mentioned previously, the characteristic peaks for zeolite MFI are between 7-9^o 2θ and 23-25^o 2θ. The peaks between 23-25^o are present line up well and show similar relative intensities. The 7-9^o does appear to be lower intensities for the samples as compared to the reference pattern. However, the reference pattern showed is a calcined sample of Si-MFI. Overall, both batches appear to have crystallized to zeolite MFI. Following XRD, we calcined batch 1 using the previously described procedure in preparation for N_2 physisorption. After calcination, the yield was determined to be 89% for batch 1 equating to 0.98 g of zeolite recovered. The N_2 physisorption isotherm is shown below in Figure 5.

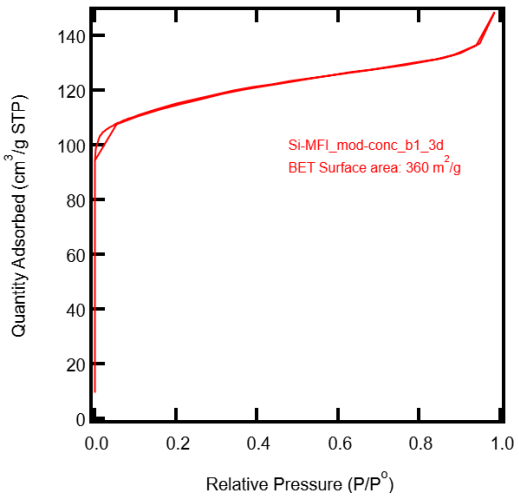

Figure 5: N_2 physisorption isotherm plot of quantity of N_2 adsorbed to the zeolite pores versus the relative pressure in the tube for Si-MFI synthesized under moderate concentrations.

Given the microporous nature of zeolites, a crystalline zeolite sample is expected to absorb primarily at low relative pressures. Figure 5 shows this in which approximately 65% of the adsorption of N_2 occurred at low relative pressures. No hysteresis appears in this data suggesting that there is minimal mesoporosity in this material. The apparent hysteresis at relative pressures below 0.1 is an artifact of the data collection. During desorption data collection, larger relative pressure drops are used when collecting data at low relative pressures. This causes this apparent hysteresis. The surface area calculated using BET theory was 360 m^2/g of the sample. Zeolite MFI has been shown to have surface areas calculated via BET theory of 350 m^2/g to 500 m^2/g [20]. Therefore, it appears that the Si-MFI sample has appropriate crystallinity and porosity characteristics of zeolite MFI.

Once XRD measurements of the Si-MFI samples synthesized at moderate concentrations were completed, we synthesized two Si-MFI batches with 0.5 wt% spermine under moderate concentrations were produced. We used the same synthesis ratios with the addition of spermine to achieve a solution weight % of 0.5%. The first batch remained in the oven for 4 days while the second batch remained in the oven for 13 days. We filtered both batches with centrifugation in the method described in the Experimental Description. Once dried, we performed XRD on these batches, and the results are shown in Figure 6.

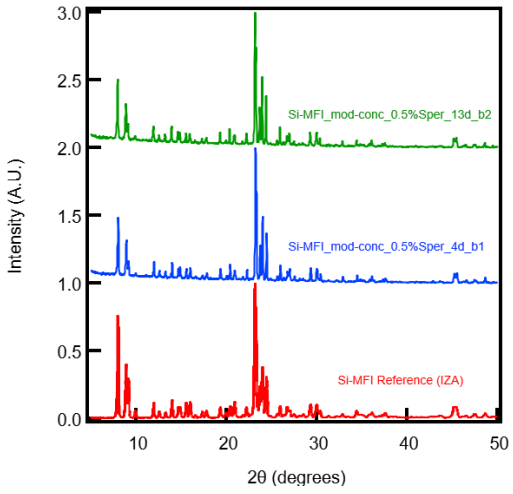

Figure 6: XRD pattern of batch 1 (blue) and batch 2 (green) of Si-MFI syntheses with 0.5% spermine against an IZA Si-MFI reference (red) [18].

Similar to the Si-MFI batches without spermine, the XRD patterns of Si-MFI with 0.5% spermine contain the peaks characteristic of Si-MFI. Additionally, the relative intensities of the 7-9^o peaks of the samples were lower than the reference pattern. However, the samples appear to be zeolite MFI from these XRD patterns. Following XRD, we calcined batch 1 to remove any

organic species remaining in the sample. The yield of zeolite was measured to be 0.70 g or 63% of the maximum possible yield. We then performed N_2 physisorption with the quantity of N_2 adsorbed versus relative pressure shown below in Figure 7.

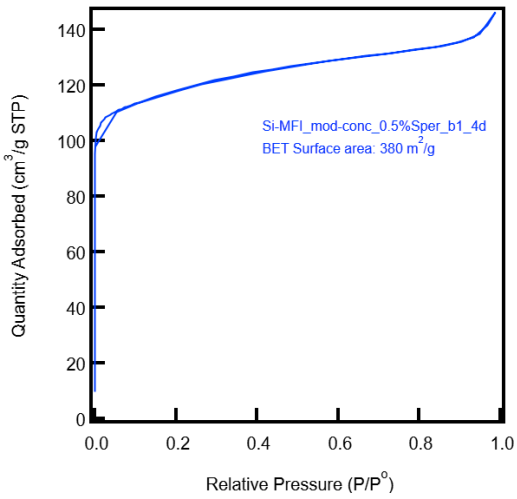

Figure 7: N_2 physisorption isotherm plot of quantity of N_2 adsorbed versus relative pressure for Si-MFI with 0.5% spermine under moderate synthesis concentrations.

The isotherm plot shown indicates that this material is highly microporous with about 65% of the adsorption occurring at very low relative pressures. From this data, the BET surface area was calculated to be 370 m^2/g of material. This surface area is within the expected range for zeolite MFI materials. Therefore, the synthesis of Si-MFI with 0.5% spermine was successful.

Because the Si-MFI syntheses were successful, we began synthesizing Sn-incorporated zeolite MFI at moderate concentrations. The synthesis ratios were 1 SiO_2 : 0.24 TPAOH : 55.6 H_2O : 4 ethanol : 0.005 $SnCl_4$. We synthesized three batches in a 160 ^oC oven. We removed the first batch from the oven after 4 days, the second batch after 16 days, and the third batch after 4 days. We filtered each batch using centrifugation and dried in the 80 ^oC oven. The XRD patterns measured for these materials are shown in Figure 8.

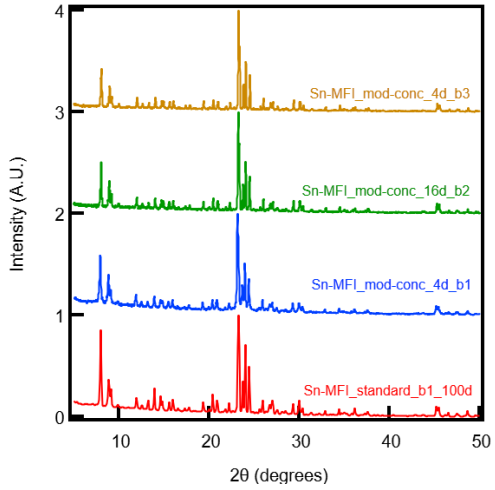

Figure 8: XRD patterns of batch 1 (blue), batch 2 (green), batch 3 (gold) of Sn-MFI under moderate synthesis concentrations versus conventional Sn-MFI (red)

In Figure 8, each sample contains the peaks in the 7-9^o and 23-25^o 2θ that are characteristic of zeolite MFI. However, the relative ratios of the peaks in the 7-9^o and 24^o 2θ regions are different for the Sn-MFI samples as compared to the reference. This suggests that there might be differing crystallization between these samples and the reference. After XRD was performed, we calcined all three batches in preparation for kinetic testing and N_2 physisorption. The yield of calcined zeolite from batch 1 was 1.01 g or 91% of the maximum yield. Batch 2 and batch 3 yielded over 80% of the maximum possible yield. To date, only batch 1 has been tested with N_2 physisorption, and the adsorbed N_2 versus relative pressure plot is shown in Figure 9.

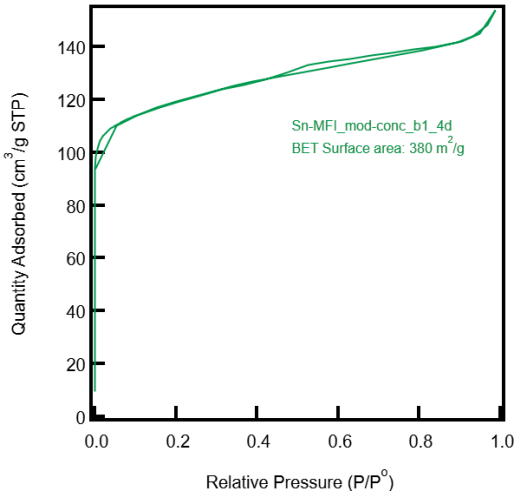

Figure 9: N_2 physisorption isotherm plot of quantity of N_2 adsorbed versus relative pressure for Sn-MFI with under moderate synthesis concentrations.

From the N_2 physisorption testing, the isotherm plot shown in Figure 9 indicates that batch 1 of this Sn-MFI sample is mostly microporous with approximately 65% of the adsorption occurring at low relative pressures. However, there is slight hysteresis between relative pressures of 0.5 and 0.8 which may indicate that the material has some mesoporosity [13]. Additionally, the BET surface area was calculated to be 380 m^2/g. Since this surface area is within the expected range for zeolite MFI materials, the Sn-MFI material was determined to be sufficiently crystalline to proceed with kinetic testing.

In tandem with Sn-MFI samples synthesized without spermine, we synthesized Sn-MFI samples with spermine to assess the effect spermine has on the catalytic and physical characteristics of the materials. We synthesized three Sn-MFI samples using a procedure similar to the Si-MFI syntheses with the addition of 0.5% spermine. We removed the first batch from the oven after 5 days, the second batch after 13 days, and the third batch after 4 days. We separated all batches using centrifugation and dried at 80^oC. We assessed the crystallinity of these uncalcined samples using XRD, and the resulting patterns are shown in Figure 10 below.

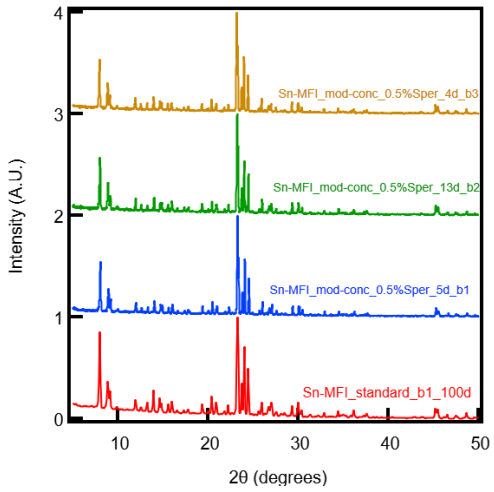

Figure 10: XRD pattern of batch 1 (blue), batch 2 (green), and batch 3 (gold) of Sn-MFI synthesized with 0.5% spermine under moderate concentrations.

Similar to the Sn-MFI batches without spermine, the peaks at 7-9^o and 23-25^o 2θ that are characteristic of zeolite MFI are present. Additionally, the relative intensities of the 7-9^o peaks and 24^o peak were different between the samples and the conventional Sn-MFI reference. However, all of the Sn-MFI samples synthesized with 0.5% spermine under moderate concentrations show consistent peak locations and relative intensities. Following XRD, we calcined all three batches. However, we have yet to perform N_2 physisorption on any Sn-MFI sample synthesized with spermine.

In summary, the zeolite MFI samples synthesized under moderate concentrations appear to be crystalline MFI samples with consistently microporous characteristics. Additional N_2 physisorption should be completed on each Sn-MFI sample since they were used for the following kinetic testing. Also, SEM should be completed on at least one batch of Si-MFI, Si-MFI with 0.5% spermine, Sn-MFI, and Sn-MFI with 0.5% spermine to assess the effects of spermine on the morphology of the zeolite crystals. Furthermore, elemental analysis should be conducted on the Sn-MFI samples to assess the amount of Sn-incorporated into these materials.

Kinetic Testing Results

To test the catalytic activity of the Sn-MFI samples produced, we used them in the kinetic testing of the epoxide ring-opening of 1,2-epoxyhexane with methanol. We produced a solution of 0.4 M 1,2-epoxyhexane with DGDE and 2.00 mL of methanol. We also used approximately 0.0385 g of each catalyst. This amount of catalyst corresponds to an epoxide : Sn ratio of 250:1 assuming a Sn-incorporation of 200 Si:1 Sn. Each set of testing was completed at 60 ^{o}C with stirring at 600 rpm. Previous work in our group demonstrated that 600 rpm was sufficient to prevent external diffusion limitations [5].

First, we used batch 1 of the Sn-MFI synthesized under moderate concentrations for kinetic testing. We collected samples of approximately 40 μL twice initially and then 15 minutes, 30 minutes, 1 hour, 2 hours, 4 hours, 7 hours, and 24 hours after we added the catalyst. We measured the ratios of components in each sample using GC-FID. The fractional conversion of 1,2-epoxyhexane is plotted for each time point in Figure 11. Using the data up to the 1-hour time point, we fit the reaction rate constant using nonlinear least squares regression. The resulting rate constant was 0.82 1/hr, and the experimental data began deviating from first-order kinetics by the 1-hour data point. By 4 hours, a the reaction achieved a fractional conversion of 0.60. By 7 hours, the reaction achieved a fractional conversion of 0.71.

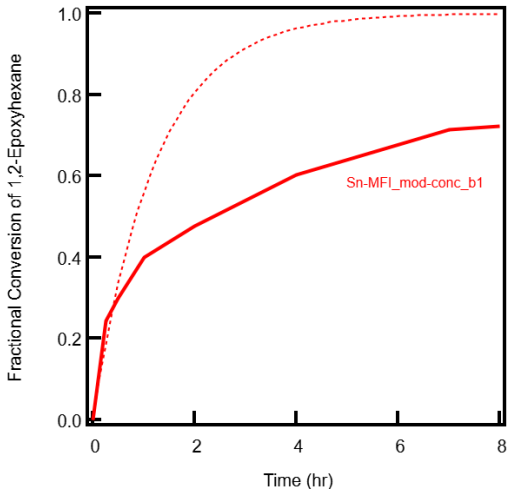

Figure 11: Conversion of 1,2-epoxyhexane using batch 1 of the Sn-MFI synthesized under moderate concentrations (solid) compared to first-order kinetics (dashed).

Next, we used batch 2 of Sn-MFI synthesized under moderate concentrations in kinetic testing. We obtained data at the same time points, and we used GC-FID to measure the ratios of the various components. We calculated the fractional conversion of 1,2-epoxyhexane plotted it versus time in Figure 12. Using data points up to the 1-hour time point, we fitted a rate constant of 0.48 1/hr. The conversions achieved by the reaction at 4 hours and 7 hours were 0.39 and 0.44, respectively. Oddly, these values indicate a significantly lower catalytic activity for Sn-MFI batch 2 despite the same synthesis procedures being used and similar XRD patterns being obtained.

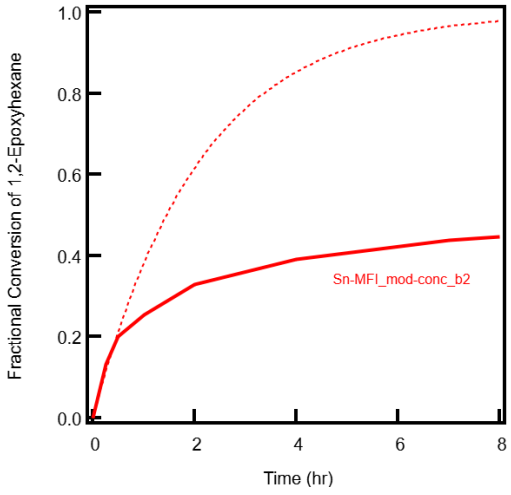

Figure 12: Conversion of 1,2-epoxyhexane using batch 2 of the Sn-MFI synthesized under moderate concentrations (solid) compared to first-order kinetics (dashed).

Following this, we tested batch 1 of the Sn-MFI synthesized with 0.5% spermine under moderate synthesis concentrations in the epoxide ring-opening reaction. We analyzed the collected samples using GC-FID. Then, we used the measured ratios of components to calculate the conversion of 1,2-epoxyhexane at each time point. The resulting conversion versus time plot is shown in Figure 13. The data points from time 0 to 1 hour were fit to the first-order kinetics model. The resulting rate constant was 0.48 1/hr. This rate constant is identical to that of Sn-MFI batch 2 (no spermine). Therefore, it seems that batch 1 of Sn-MFI (no spermine) had significantly higher catalytic activity. Additionally, the conversions achieved using batch 1 of Sn-MFI synthesized with spermine at 4 hours and 7 hours were 0.35 and 0.38, respectively. Therefore, the spermine sample achieved lower conversions than the non-spermine sample despite having the same initial rate constant.

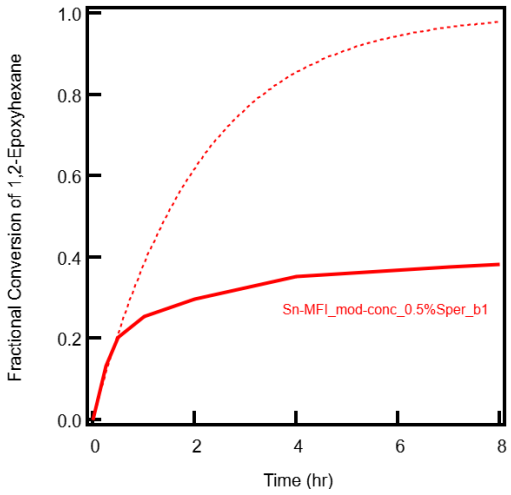

Figure 13: Conversion of 1,2-epoxyhexane using batch 1 of the Sn-MFI synthesized with 0.5% spermine under moderate concentrations (solid) compared to first-order kinetics (dashed).

Additionally, we also tested the third batch of Sn-MFI synthesized with 0.5% spermine. Throughout this test, the silica filters were not able to completely filter the catalyst from the samples. Therefore, some samples took multiple filters to separate the catalyst fully. The fractional conversions calculated using reaction mixture analysis are plotted versus time in Figure 14. Oddly, no conversion was achieved between the 2- and 4-hour time points. This could be due to inaccurate sampling or residual catalyst remaining in the filtered sample. Fitting this data through the time point using the first-order kinetics model yielded a rate constant of 0.45 1/hr. Additionally, the 4-hour and 7-hour conversions achieved were 0.34 and 0.38, respectively.

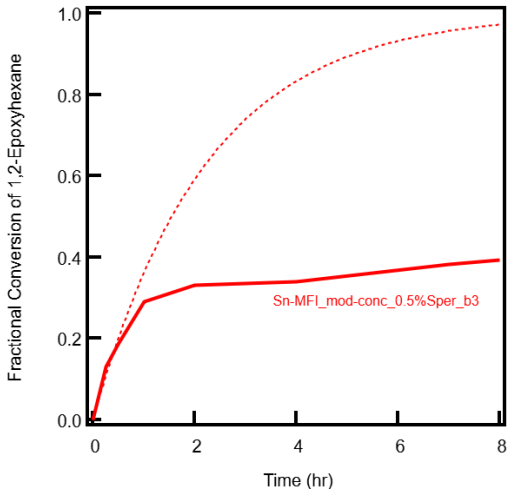

Figure 14: Conversion of 1,2-epoxyhexane using batch 3 of the Sn-MFI synthesized with 0.5% spermine under moderate concentrations (solid) compared to first-order kinetics (dashed).

Finally, we tested the third batch of Sn-MFI synthesized without spermine in the epoxide ring-opening reaction. We calculated the conversions using the methods described previously and were plotted versus time in Figure 15. The first-order reaction kinetics model was fit to the data through the time point. The resulting rate constant was 0.53 1/hr with conversions of 0.42 after 4 hours and 0.54 after 7 hours.

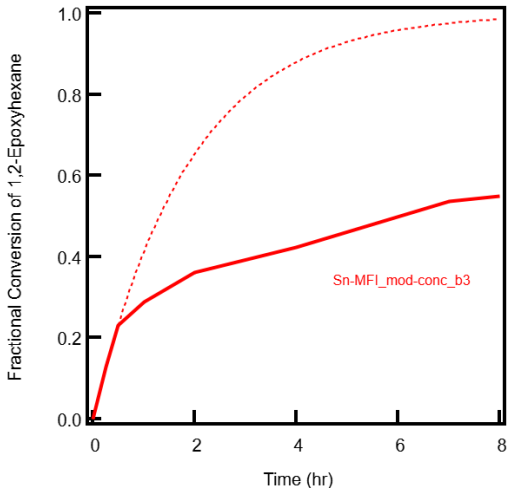

Figure 15: Conversion of 1,2-epoxyhexane using batch 3 of the Sn-MFI synthesized under moderate concentrations (solid) compared to first-order kinetics (dashed).

In total, we tested three samples of Sn-MFI synthesized without spermine and two samples synthesized with spermine. Additional testing is being completed to generate more data points.

However, the summary of the kinetic testing of the five samples successfully run is shown in Table 2. The table contains the reaction rate constants (k), the fractional conversion after 4 hours, and the fractional conversion after 7 hours for each sample.

Table 2: Kinetic testing results for Sn-MFI tested with and without spermine.

Sample	k (hr^{-1})	Conversion, 4 hours	Conversion, 7 hours
Sn-MFI_mod-conc_b1	0.82	0.60	0.71
Sn-MFI_mod-conc_b2	0.48	0.39	0.44
Sn-MFI_mod-conc_0.5%Sper_b1	0.48	0.35	0.38
Sn-MFI_mod-conc_0.5%Sper_b3	0.45	0.34	0.38
Sn-MFI_mod-conc_b3	0.53	0.42	0.54

To determine if there is a statistical difference between the Sn-MFI with and without spermine for the reaction rate constants, the conversion after 4 hours, or the conversion after 7 hours, we performed t-tests on the kinetic testing data. The null hypothesis for the reaction rate constant statistical test was that the means of the rate constants of the non-spermine Sn-MFI samples and spermine Sn-MFI samples were not statistically different from each other. We used similar hypotheses for the 4-hour conversion and 7-hour conversion. For these statistical tests, we used a significance value of 0.05. The resulting p-values were 0.37 for the rate constants, 0.24 for the 4-hour conversions, and 0.17 for the 7-hour conversions. Since all of the p-values were greater than the significance level, we cannot reject the null hypothesis. In other words, our data suggests that samples synthesized with 0.5% spermine are not catalytically different from samples synthesized without spermine.

However, additional testing should be conducted to add further resolution to the statistical tests. One potential way to directly compare the catalytic performance of these materials is to use less diffusionally limited epoxides. For example, epichlorohydrin has been shown to be less diffusionally limited in Lewis acid zeolite catalysis within our group. With fewer diffusion limitations, kinetic testing data using epichlorohydrin varies less from first-order kinetics. Tests using this epoxide may be able to reveal any effects spermine has on the catalytic activity, Sn-incorporation, or active sites in Sn-MFI materials. Additionally, elemental analysis should be conducted to directly determine if spermine affects the Sn-incorporation of these materials. SEM should also be used to determine if the added spermine actually modified the morphology of the zeolite samples. Finally, testing with additional spermine concentrations and different total synthesis solution concentrations should be investigated to understand the role of these variables.

Conclusions

In summary, the dilute synthesis conditions suggested in Rimer et al. produced zeolite MFI under a 1 SiO_2 : 1 TPAOH : 233 H_2O : 4 Ethanol synthesis ratio. The crystals we produced were large enough to filter using vacuum filtration. However, the low synthesis concentrations yielded small amounts of zeolite whether the ZGM spermine was used or not. The yields were too low to characterize the materials via N_2 physisorption, SEM, or kinetic testing.

As a result, we used more moderate concentrations. In the end, synthesis ratios of 1 SiO_2 : 0.24 TPAOH : 55.6 H_2O : 4 Ethanol were used. For syntheses involving spermine, we added enough spermine to achieve a total synthesis solution spermine weight % of 0.05%. For Sn-MFI samples, the Si:Sn ratio was 1:0.005. XRD confirmed that all samples synthesized under moderate concentrations were crystalline zeolite MFI. Additionally, N_2 physisorption suggested that the zeolites synthesized were primarily microporous with BET surface areas between 360 and 380 m^2/g of material. Overall, zeolites were successfully synthesized at moderate solution concentrations of 1 SiO_2 : 55.6 H_2O with and without spermine.

Following the successful synthesis of zeolite MFI under moderate synthesis concentrations, the Sn-MFI samples synthesized without spermine and the Sn-MFI samples synthesized with spermine underwent kinetic testing. We used these Lewis acid catalysts to catalyze the reaction of 1,2-epoxyhexane using excess methanol. We measured the conversions of 1,2-epoxyhexane over 24-hour periods. Using this data, first-order reaction rate constants were fitted using nonlinear least-squares regression for the data points up to 1 hour. By comparing the reaction rate constants, conversions at 4 hours, and conversions at 7 hours, we determined that there was not a significant difference in the catalytic activity of Sn-MFI samples synthesized with spermine compared to those synthesized without spermine.

However, only five total trials of kinetic testing were performed. We recommend additional trials of kinetic testing to refine the power of the statistical tests. Additionally, kinetic testing should be performed with epichlorohydrin since this reactant has fewer diffusion limitations. This may provide additional ability to differentiate between the catalytic activity of Sn-MFI samples synthesized with and without spermine. Additional N_2 physisorption tests should be performed to assess the porosity of all Sn-MFI samples. SEM should also be performed to determine if the spermine modified the morphology of the Sn-MFI samples as Rimer et al. had previously shown.

In summary, zeolites provide unparalleled abilities to combine high catalytic activities, ease of separation, and selectivity. However, methods to modify the morphology of zeolite crystals are needed to decrease diffusion limitations that plague these materials. Since the addition

of 0.5 weight % spermine to synthesis solutions was shown to not affect the catalytic activity and decrease diffusion limitations, other methods to modify Sn-MFI morphology may be more viable. For example, the fluorinated silica precursors used by Vatlchev et al. could be used to adjust the morphology of MFI crystals. Additionally, decreasing one dimension down to the nanoscale to make Sn-MFI nanosheets may be necessary. As such, these routes should be pursued to maximize the catalytic activity of zeolite materials.

References

1. Carraher, J. M., Fleitman, C. N. & Tessonnier, J.-P. Kinetic and mechanistic study of glucose isomerization using homogeneous organic Brønsted base catalysts in water. *ACS Catalysis* **5,** 3162–3173 (2015).
2. Herrmann, W. A. & Kohlpaintner, C. W. Water-soluble ligands, metal complexes, and catalysts: synergism of homogeneous and heterogeneous catalysis. *Angewandte Chemie International Edition in English* **32,** 1524–1544 (1993).
3. Deshpande, N. *et al.* Selectively converting glucose to fructose using immobilized tertiary amines. *Journal of Catalysis* **353,** 205–210 (2017).
4. Grasselli, R. K. Advances and future trends in selective oxidation and ammoxidation catalysis. *Catalysis Today* **49,** 141–153 (1999).
5. Deshpande, N. *et al.* Epoxide ring opening with alcohols using heterogeneous Lewis acid catalysts: Regioselectivity and mechanism. *Journal of Catalysis* **370,** 46–54 (2019).
6. Deshpande, N., Cho, E. H., Spanos, A. P., Lin, L.-C. & Brunelli, N. A. Tuning molecular structure of tertiary amine catalysts for glucose isomerization. *Journal of Catalysis* **372,** 119–127 (2019).
7. Olson, D., Kokotailo, G., Lawton, S. & Meier, W. Crystal structure and structure-related properties of ZSM-5. *The Journal of Physical Chemistry* **85,** 2238–2243 (1981).
8. Parulkar, A., Spanos, A. P., Deshpande, N. & Brunelli, N. A. Synthesis and catalytic testing of Lewis acidic nano zeolite Beta for epoxide ring opening with alcohols. *Applied Catalysis A: General* **577,** 28–34 (2019).
9. Larlus, O. & Valtchev, V. Synthesis of all-silica BEA-type material in basic media. *Microporous and mesoporous materials* **93,** 55–61 (2006).
10. Lupulescu, A. I., Kumar, M. & Rimer, J. D. A facile strategy to design zeolite L crystals with tunable morphology and surface architecture. *Journal of the American Chemical Society* **135,** 6608–6617 (2013).
11. Lupulescu, A. I. & Rimer, J. D. Tailoring Silicalite-1 Crystal Morphology with Molecular Modifiers. *Angewandte Chemie* **124,** 3401–3405 (2012).
12. Dai, W. *et al.* Platelike MFI Crystals with Controlled Crystal Faces Aspect Ratio. *Journal of the American Chemical Society* **143,** 1993–2004 (2021).

13. Sing, K. S. Reporting physisorption data for gas/solid systems with special reference to the determination of surface area and porosity (Recommendations 1984). *Pure and applied chemistry* **57,** 603–619 (1985).

14. Sing, K. The use of nitrogen adsorption for the characterisation of porous materials. *Colloids and Surfaces A: Physicochemical and Engineering Aspects* **187,** 3–9 (2001).

15. Rawlings, J. & Ekerdt, J. *Chemical Reactor Analysis and Desing Fundamentals* 2nd ed., pg. 523 (Nob Hill Publishing, Wisconsin, 2002).

16. Van Embden, J., Sader, J. E., Davidson, M. & Mulvaney, P. Evolution of colloidal nanocrystals: theory and modeling of their nucleation and growth. *The Journal of Physical Chemistry C* **113,** 16342–16355 (2009).

17. Mintova, S., Gilson, J.-P. & Valtchev, V. Advances in nanosized zeolites. *Nanoscale* **5,** 6693–6703 (2013).

18. Baerlocher, C. & McCusker, L. *Database of Zeolite Structures* `http://www.iza-structure.org/databases/`.

19. *Verified Syntheses of Zeolitic Materials* 2nd (eds Robson, H. & Lillerud, K.) **4-6,** 198–199. ISBN: 978-0-444-50703-7 (Elsevier BV, 2001).

20. Yuan, E. *et al.* Facile synthesis of Sn-containing MFI zeolites as versatile solid acid catalysts. *Microporous and Mesoporous Materials* **270,** 265–273 (2018).

Appendix A: Synthesis Details

Table 3: Masses of TEOS, TPAOH, H_2O, $SnCl_4$, and spermine added for each sample.

Material	Max SiO_2 yield (g)	TEOS (g)	TPAOH (g)	H_2O (g)	$SnCl_4$ (g)	Spermine (g)
Si-MFI_standard	1.80	6.38	2.2	11.46	0	0
Sn-MFI_standard	1.80	6.38	2.2	11.46	0.0537	0
Si-MFI_dil	0.30	1.10	2.62	20.28	0	0
Si-MFI_dil_0.5%Sper	0.30	1.10	2.62	20.28	0	0.124
Sn-MFI_dil	0.30	1.10	2.62	20.28	0.0092	0
Si-MFI_mod-conc	1.11	3.92	2.25	17.82	0	0
Si-MFI_mod-conc_0.5%Sper	1.11	3.92	2.25	17.82	0	0.124
Sn-MFI_mod-conc	1.11	3.92	2.25	17.82	0.0330	0
Sn-MFI_mod-conc_0.5%Sper	1.11	3.92	2.25	17.82	0.0330	0.124

Table 4: Summary of each zeolite batch.

Sample Type	Days in oven	Heteroatom	Modifier	% Mass Yield
Si-MFI_dil_0.5%Sper_b1	3	–	0.5 wt% Spermine	Insufficient
Si-MFI_dil_0.5%Sper_b2	11	–	0.5 wt% Spermine	Low
Si-MFI_dil_0.5%Sper_b3	16	–	0.5 wt% Spermine	Low
Sn-MFI_dil_b1	14	1 Si: 0.005 Sn	–	Low
Si-MFI_dil_0.5%Sper_b4	22	–	0.5 wt% Spermine	9%
Sn-MFI_dil_b2	58	1 Si: 0.005 Sn	–	54%
Si-MFI_dil_b1	41	–	–	Low
Si-MFI_mod-conc_b1	3	–	–	89%
Si-MFI_mod-conc_b2	17	–	–	
Si-MFI_mod-conc_0.5%Sper_b1	4	–	0.5 wt% Spermine	63%
Si-MFI_mod-conc_0.5%Sper_b2	13	–	0.5 wt% Spermine	
Sn-MFI_mod-conc_b1	4	1 Si: 0.005 Sn	–	91%
Sn-MFI_mod-conc_b2	16	1 Si: 0.005 Sn	–	>80%
Sn-MFI_mod-conc_0.5%Sper_b1	5	1 Si: 0.005 Sn	0.5 wt% Spermine	>80%
Sn-MFI_mod-conc_0.5%Sper_b2	13	1 Si: 0.005 Sn	0.5 wt% Spermine	>80%
Sn-MFI_mod-conc_b3	4	1 Si: 0.005 Sn	–	>80%
Sn-MFI_mod-conc_0.5%Sper_b3	4	1 Si: 0.005 Sn	0.5 wt% Spermine	>80%